S-shaped Double Helicene Diimides: Synthesis, Self-assembly, and Mechanofluorochromism

Guanghui Zhang[#1], Jingyun Tan[#1,2], Long Zhou[1], Jun Liu[1], Chao Liu[1], Yingping Zou[1], Akimitsu Narita[2], Yunbin Hu*[1]

[1] College of Chemistry and Chemical Engineering, Central South University, Changsha, Hunan 410083, P. R. China;

[2] Organic and Carbon Nanomaterials Unit, Okinawa Institute of Science and Technology Graduate University, 1919-1 Tancha, Onna-son, Kunigami-gun, Okinawa 904-0495, Japan.

Supporting Information Placeholder

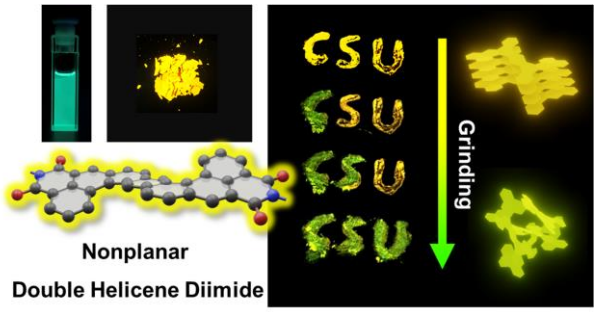

ABSTRACT: Herein, we present a synthesis of S-shaped double helicene with fused imide moieties, achieving a contorted aromatic diimide (**DHDI**) with good fluorescence properties both in solution and solid states. **DHDI** demonstrates distinct mechanofluorochromism from yellow to green emission under grinding of its crystalline powder.

Molecular assembly driven by intermolecular noncovalent interactions plays a critical role on the bulk properties of functional organic materials.[1] Among various noncovalent interactions, π - π interactions are prominent in aromatic systems, giving rise to intriguing properties such as charge-carrier transport,[2] luminescence,[3] mechanochromism,[4] and thermal expansion.[5] Nevertheless, excessive π - π interactions can lead to poor solubility and aggregation caused quenching (ACQ) of fluorescence, which restrict their applications.[6] Therefore, modulation of the degree of π - π interaction at the molecular level is a fundamental research issue.

The planarity of aromatic core structure is an important factor for adjusting the intermolecular interactions. In particular, nonplanar structures have been demonstrated to suppress the π - π interactions, thus enhancing the solubility of large polycyclic aromatic hydrocarbons (PAHs).[7] Helicene, featuring *ortho*-fused benzene rings, is a prototypical class of contorted PAHs.[8] The unique helical conjugation of helicenes give rise to their compelling potentials in wide range of areas, for example, as nonlinear optical materials,[9] organic semiconductors,[10] molecular sensors,[11] and molecular motors.[12] Early researches mainly focused on pristine carbohelicenes.[13] Nevertheless, the fluorescence quantum yields of such all-carbon helicenes are not satisfactory for applications in optoelectronics, due to relatively low radiative rate upon photoexcitation.[14] Core-modified helicenes have emerged as the alternatives either with heteroatom-incorporation into the aromatic backbone or decoration of peripheral positions of the main scaffold with functional groups, which are more desired to achieve tunable photophysical properties.[15] Imide group is considered as a promising fluorophore unit that was used to merge with polyaromatic cores, affording versatile aromatic imides such as the well-known perylene diimide (Figure 1a).[16] Despite the intrinsic fluorescence, the emission of planar aromatic imides with extended π -conjugation easily suffer from the ACQ effect due to the aggregation by the strong π - π interactions.[17]

Accordingly, the fusion of helicene with imide units is an attractive combination to construct nonplanar aromatic imides with enhanced fluorescence both in solution and solid state. For example, Sakai *et.al* fused [5]helicene with a maleimide unit. The fluorescence quantum yield (Φ) of the resulting compound (Φ = 37%) was almost tenfold increment compared with the all-carbon analogue (Φ = 4%).[18] Recently, Ravat *et.al* reported a novel class of helicene diimide by merging [n]helicene skeleton with two imide units, showing good emission properties both in solution and solid state (Φ = 22% and 17%, respectively).[19] Considering the solid-state emission and flexible molecular packing, helicene imide derivatives might exhibit promising mechanofluorochromic behaviors,[20] that is, the emission color switching in response

to external mechanical stimuli because of the perturbation of molecular packing. However, this intriguing property of helicene imides still remains unexplored. In this context, we herein report a novel double helicene diimide (**DHDI)** via the lateral fusion of S-shaped double [4]helicene by two imide segments (Figure 1b). [4]Helicene owns relatively small dihedral angles between terminal benzene rings compared to the higher helicene homologues (Figure 1c),[21] which suggests that the planarity of the π-conjugated structure could still be retained to maintain adequate π - π interactions for molecular stacking and, ultimately, triggering mechanofluorochromic behavior.

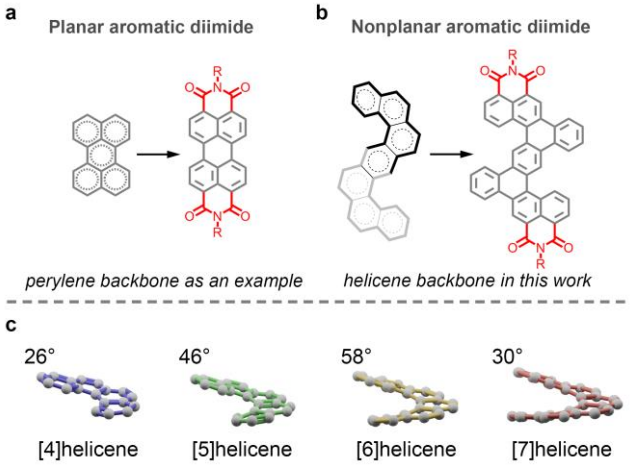

Figure 1. a) Structure of planar aromatic diimide; b) Structure of nonplanar aromatic diimide based on S-shaped double [4]helicene backbone in this work; c) The dihedral angles between both terminal benzene moieties of different helicenes.[21]

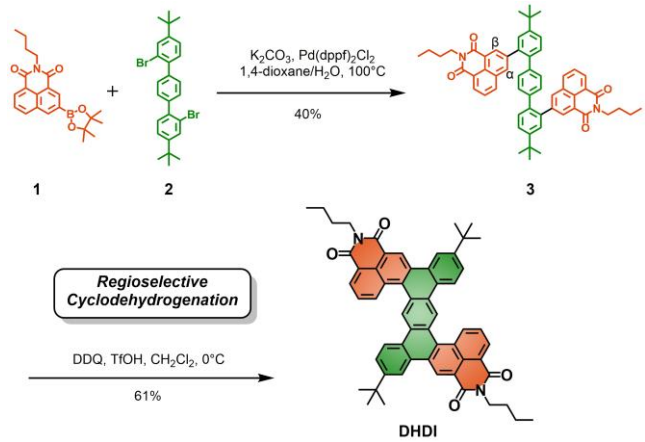

Scheme 1. The synthetic route to helicene diimide **DHDI**. (DDQ: 2,3-Dichloro-5,6-dicyano-1,4-benzoquinone; TfOH: trifluoromethanesulfonic acid)

The synthesis of **DHDI** was designed with one key annulation procedure based on regioselective Scholl reaction (Scheme 1).[22] The key precursor **3** was synthesized via Suzuki-Miyaura cross-coupling between boronic ester **1** and dibromo-*p*-terphenyl **2** with yield of 40% (See SI for the synthesis details of **1** and **2**). Then, the two-fold oxidative cyclodehydrogenation of **3** selectively took place at α-positions of the naphthylimide subunits, resulting in the formation of **DHDI** as yellow solid with yield of 61%. The regioselectivity is likely caused by the higher electron density and less steric hindrance of the α-position over the β-position of **3**, which is in line with reported cases of twisted polycyclic diimides.[23] Apart from ^{1}H and ^{13}C NMR and mass spectra, the structure of **DHDI** was further ascertained by ^{1}H – ^{1}H correlation spectroscopy (COSY) and nuclear overhauser enhancement spectroscopy (NOESY) measurements (Figure S1).

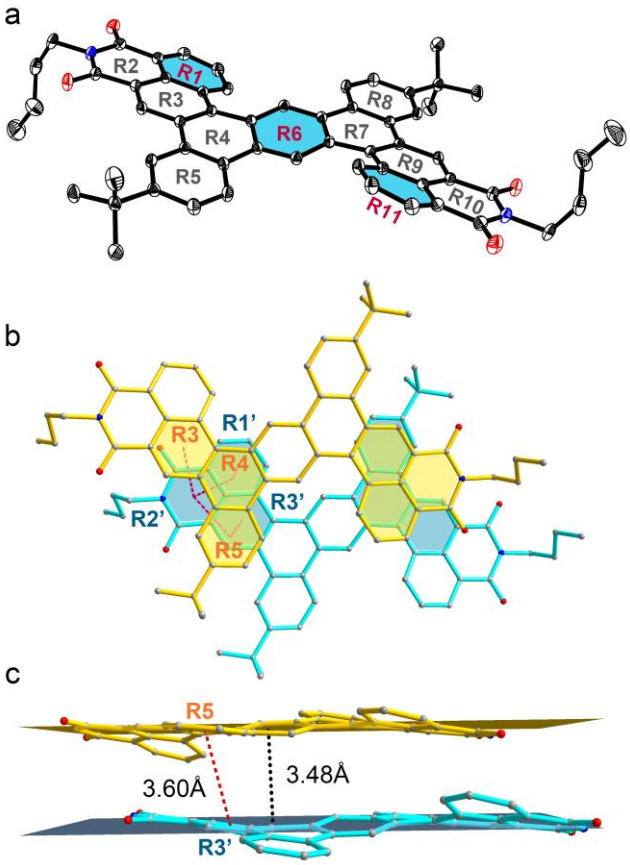

Figure 2. a) The ORTEP diagram of **DHDI** (50% probability displacement ellipsoids for non-H atoms; CCDC no. 2058085); b) c) The π - π packing pattern from top view and side view, respectively. For clarity, the hydrogen atoms and side chain such as *n*-butyl and *t*-butyl groups are omitted as needed.

Single crystal suitable for X-ray crystallography analysis was obtained by slow evaporation of a solution of **DHDI** in dichloromethane/toluene (see SI). The single-crystal X-ray analysis unambiguously confirms the S-shaped steric structure of **DHDI**, as shown by the ORTEP diagram (Figure 2a, Figure S3). Detailed parameters for crystal data and structure refinement, selected bond length, bond angle, torsion angle and dihedral angle are reported in Table S1 and S2. The torsions of the two [4]helicene subunits, defined by the dihedral angles of terminal rings R1/R6 and R6/R11, are 21.97° and 29.20° , respectively. These values are comparable to that of [4]helicene (26°). To evaluate the distortion of this helical backbone more subtly, the average value of dihedral angles between adjacent rings (θ_a) was also calculated.[24] The parameter θ_a for representive [4]helicene,[25] [5]helicene,[26] [6]helicene[27] and [7]helicene[28] is 9.81° , 12.61° , 13.37° and 11.92° , respectively. The θ_a value of **DHDI** is 8.68° , indicating that the molecular backbone is only slightly contorted. The molecular packing in the crystal structure (Figure 2b and 2c) displays slipped π - π stacking pattern with the average π - π stacking distance of 3.48 Å, as

determined by the distance between the mean planes of molecular backbones. Distinct π - π stacking contacts can be found between fused benzene rings R1′ /R2′ /R3′ and aromatic imide rings R3/R4/R5. The shortest distance of ring centroid is 3.60Å (R3′ -R5). It should be noted that, due to the contorted structure and steric hindrance, the overall overlap of two adjacent molecules is relatively small, indicating partial π - π interactions.

To gain further insight into the intermolecular interactions, we studied the self-assembly behaviors of **DHDI** in solution by analyzing the ^{1}H NMR spectroscopy under varying concentration. As shown in Figure S3 and S4, the signal of aromatic protons shifted to upfield with the concentration increased from 1.25 × 10^{-4} M to 1.25 × 10^{-2} M. This phenomenon is likely due to self-association of **DHDI** in solution. The association constant (K_{assoc}) was calculated by the isodesmic model with the equal constant assumption (See SI for detailed definition and calculation).[29] The fitted dilution curves for **DHDI** are shown in Figure S5 and the detailed fitting parameters are reported in Table S3. The average K_{assoc} was estimated to be 43.7 M^{-1}, which is lower than that of the previously reported cyclobis[4]helicene (K_{assoc} = 64.9 M^{-1}).[29b]

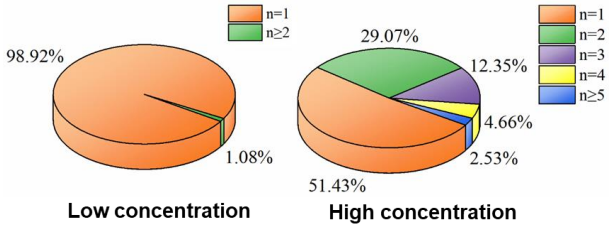

Figure 3. Self-assembly behavior of **DHDI**. Populations of oligomeric n-mers in terms of mass fractions under low and high concentration (1.25 × 10^{-4} M and 1.25 × 10^{-2} M, respectively).

The mass fractions of different oligomers are calculated to obtain concrete insight of the population of oligomeric n-mers (Figure 3, see SI for details of the calculation).[29c] Under the lowest concentration (1.25 × 10^{-4} M), almost all **DHDI** molecules are present as a monomer (fraction = 98.92%). Upon increasing the concentration by 100-fold (1.25 × 10^{-2} M), the fraction of dimer reaches 29.07%, while the proportion of monomer decreases (fraction = 51.43%). Despite the reduction, the monomer is still the predominate component. The result implies the molecular structure with the contorted backbone and the peripheral *n*-butyl and *t*-butyl groups, which inducing the steric hindrance introduced by surrounding the aromatic core, endow **DHDI** good solubility and low tendency of assembly.

The photophysical property of **DHDI** was investigated by UV-Vis absorption and fluorescence spectroscopies as well as theoretical calculation. Taking the result in dichloromethane as example, **DHDI** shows a low-energy absorption band from 375 to 500 nm, with the maximum peak at 445 nm and a shoulder at 424 nm (Figure 4a). According to time-dependent density functional theory (TD-DFT) calculation, the low-energy absorption band could be assigned mainly to the contribution of HOMO-1→LUMO transition, showing distinct intramolecular charge transfer (ICT) from double helicene core to the imide moieties (Figure S6, S7 and Table S4). In dichloromethane solution, **DHDI** displayed strong green fluorescence with a broad emission band from 450 to 650 nm peaking at 491 nm (Figure 4a). Notably, the fluorescence of **DHDI** exhibited strong solvatochromic effect with significant bathochromic shifts upon increasing the solvent polarity from hexane to dimethyl sulfoxide (Figure 4b, Figure S9, Table S5), while the UV-vis absorption showed no obvious shifts (Figure S8). The fluorescence color markedly changed from blue to green as shown in Figure 4b. This pronounced effect is explained by better stabilization of the excited state with increasing solvent polarity.[30] The absolute fluorescence quantum yield in solution was measured up to 47% (toluene), which is higher than those of conventional [4]carbohelicenes (usually around 20%).[14a, 31] In addition, the radiative decay rates of DHDI in toluene was calculated as 6.15 × 10^7 s^{-1}, which is larger than pristine [4]helicene (0.51 × 10^7 s^{-1}, obtained based on the reported value of fluorescence quantum yield and lifetime).[14a] Therefore, the combination of the S-shaped helicene backbone and imide moiety increased the radiative decay rates, which eventually enhance the fluorescence of DHDI. It also could be demonstrated by comparision with other two reference structure **r1** and **[4]helicene** based on TD-DFT calculation (Figure S10, Table S6, see SI for the detailed discussion). Moreover, **DHDI** maintained moderate emission in aggregation state with a powder fluorescence quantum yield of 18%, which could be rationalized by the slipped and partial π - π overlaps upon aggregation as revealed from the above crystallography analysis.

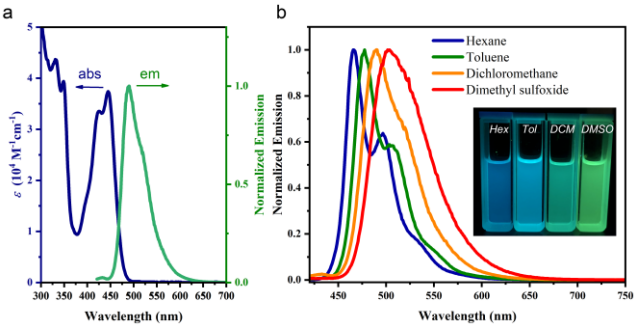

Figure 4. Photophysical properties of **DHDI**. a) UV-Vis absorption and normalized emission spectra in dichloromethane; b) Normalized emission spectra in different solvents (the inset shows the photograph under 365 nm UV light). All experiments were performed under concentration of 1.0 × 10^{-5} mol L^{-1}.

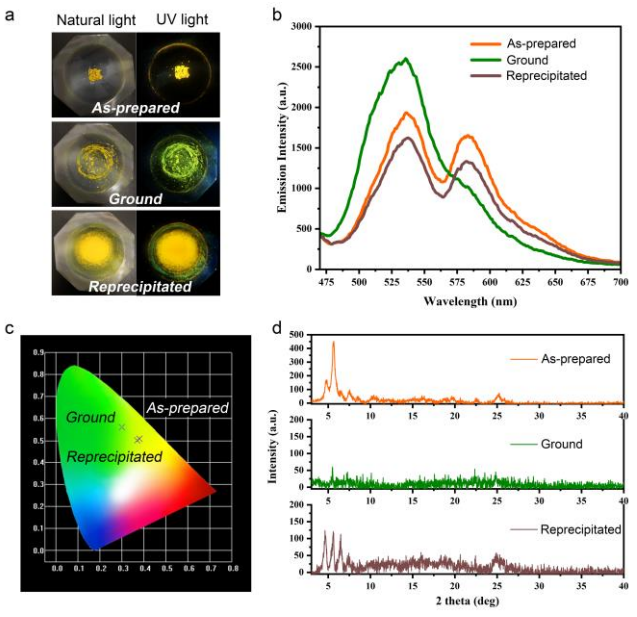

Figure 5. The mechanofluorochromism of **DHDI**. a) The photograph of as-prepared, ground, and reprecipitated powder under natural light and 365 nm UV light; b) The fluorescence spectra, c) the CIE coordinates of emission spectra and d) PXRD profiles of as-prepared, ground, and reprecipitated powder.

The partially π-stacked molecular assembly and good solid-state emission of **DHDI** evoked our interest to study its possible mechanofluorochromism. As shown in Figure 5, the as-prepared powder sample exhibited yellow fluorescence with double emission peaks at 538 and 580 nm. Upon grinding the powder, the emission color switched to green along with significant decrease of the long-wavelength emission peak at 580 nm. It's could be inferred that this emission band (580 nm) is assigned to the long range well-organized stacking structure, which is sensitive to external force. The initial yellow emissive state was quickly reproduced by re-precipitation of the ground sample from dichloromethane/acetonitrile. The mechanism of mechanofluorochromism was further studied via powder X-ray diffraction (PXRD). The PXRD pattern of as-prepared powder has a good agreement with the simulated results from the single crystal analysis (Figure S11). When the as-prepared powder was ground, the sharp peaks around 5° disappeared (Figure 5d). It could be inferred that the grinding operation broke the crystalline packing and led to amorphous powder. During the process, the long range well-organized π - π stacking interactions vanished, resulting in the hypsochromic shift of emission color.[32] The re-precipitation realigned the molecular assembly and enhanced the PXRD peaks, which was consistent with the recovery of the initial yellow emission.

To conclude, we demonstrated the facile synthesis of a nonplanar helicene diimide **DHDI** via a regioselective cyclodehydrogenation. The slightly contorted backbone of **DHDI** was unambiguously confirmed by X-ray crystallography, leading to slipped intermolecular stacking with partial π - π overlaps. The molecular assembly behavior in solution was investigated by concentration-dependent NMR spectroscopy, showing moderate aggregate tendency. The fluorescence quantum yield of **DHDI** in solution and solid were up to 47% and 18%, respectively, highlighting the advantage of the fusion of double helicene and imide to suppress the ACQ. More importantly, **DHDI** is sensitive towards mechanical force with remarkable mechanofluorochromic behavior, suggesting the potential applications in mechanosensors, security papers, and optical storage.[33] Further endeavor towards the elucidation of the intrinsic mechanism of mechanofluorochromism, as well as exploration of the functionalization and applications of **DHDI** are ongoing in our laboratory.

ASSOCIATED CONTENT

Supporting Information

The Supporting Information is available free of charge on the ACS Publications website.

Detailed experimental procedures characterization, crystallographic data, DFT calculations, photophysical properties, HRMS, and NMR spectra (PDF). FAIR Data is available as Supporting Information for Publication and includes the primary NMR FID files for compounds [1, 2, 3, DHDI].

Accession Codes

CCDC 2058085 contains the supplementary crystallographic data for this paper. These data can be obtained free of charge via www.ccdc.cam.ac.uk/data_request/cif, or by emailing data_request@ccdc.cam.ac.uk, or by contacting The Cambridge Crystallographic Data Centre, 12 Union Road, Cambridge CB2 1EZ, UK; fax: +44 1223 336033.

AUTHOR INFORMATION

Corresponding Author

Yunbin Hu−Email: huyunbin@csu.edu.cn

Author Contributions

[#]G. Zhang and J. Tan contributed equally to this work.

Notes

The authors declare no competing financial interest.

ACKNOWLEDGMENT

This work was financially supported by the National Natural Science Foundation of China (No. 21901257), Innovation-Driven Project of Central South University (No. 502501009), and the Okinawa Institute of Science and Technology Graduate University.

REFERENCES

(1) (a) Hoeben, F.J.; Jonkheijm, P.; Meijer, E.; Schenning, A.P. *Chem. Rev.* **2005,** *105*, 1491-1546; (b) Liu, K.; Kang, Y.; Wang, Z.; Zhang, X. *Adv. Mater.* **2013,** *25*, 5530-5548; (c) Stupp, S.I.; Palmer, L.C. *Chem. Mater.* **2014,** *26*, 507-518; (d) Sutton, C.; Risko, C.; Brédas, J.-L. *Chem. Mater.* **2016,** *28*, 3-16; (e) Savyasachi, A.J.; Kotova, O.; Shanmugaraju, S.; Bradberry, S.J.; Ó' Máille, G.M.; Gunnlaugsson, T. *Chem* **2017,** *3*, 764-811; (f) Krieg, E.; Niazov-Elkan, A.; Cohen, E.; Tsarfati, Y.; Rybtchinski, B. *Acc. Chem. Res.* **2019,** *52*, 2634-2646; (g) Seifrid, M.T.; Reddy, G.N.M.; Zhou, C.; Chmelka, B.F.; Bazan, G.C. *J. Am. Chem. Soc.* **2019,** *141*, 5078-5082; (h) MacFarlane, L.R.; Shaikh, H.; Garcia-Hernandez, J.D.; Vespa, M.; Fukui, T.; Manners, I. *Nature* **2020,** *41578*, 020-00233.

(2) (a) Feng, X.; Sosa-Vargas, L.; Umadevi, S.; Mori, T.; Shimizu, Y.; Hegmann, T. *Adv. Funct. Mater.* **2015,** *25*, 1180-1192; (b) Shi, D.; Qin, X.; Li, Y.; He, Y.; Zhong, C.; Pan, J.; Dong, H.; Xu, W.; Li, T.; Hu, W.; Brédas, J.-L.; Bakr, O.M. *Sci. Adv.* **2016,** *2*, e1501491; (c) Kim, Y.; Hwang, H.; Kim, N.-K.; Hwang, K.; Park, J.-J.; Shin, G.-I.; Kim, D.-Y. *Adv. Mater.* **2018,** *30*, 1706557.

(3) (a) Wang, J.-F.; Yao, Y.; Ning, Y.; Meng, Y.-S.; Hou, C.-L.; Zhang, J.; Zhang, J.-L. *Org. Chem. Front.* **2018,** *5*, 1877-1885; (b) Li, Y.; Liu, S.; Ni, H.; Zhang, H.; Zhang, H.; Chuah, C.; Ma, C.; Wong, K.S.; Lam, J.W.Y.; Kwok, R.T.K.; Qian, J.; Lu, X.; Tang, B.Z. *Angew. Chem. Int. Ed.* **2020,** *59*, 12822-12826; (c) Nitti, A.; Pasini, D. *Adv. Mater.* **2020,** *32*, 1908021.

(4) (a) Mizukami, S.; Houjou, H.; Sugaya, K.; Koyama, E.; Tokuhisa, H.; Sasaki, T.; Kanesato, M. *Chem. Mater.* **2005,** *17*, 50-56; (b) Mo, S.; Meng, Q.; Wan, S.; Su, Z.; Yan, H.; Tang, B.Z.; Yin, M. *Adv. Funct. Mater.* **2017,** *27*, 1701210; (c) Yang, W.; Liu, C.; Lu, S.; Du, J.; Gao, Q.; Zhang, R.; Liu, Y.; Yang, C. *J. Mater. Chem. C* **2018,** *6*, 290-298; (d) Zhang, Y.; Zhu, C.; Luo, Q.; Shen, Y.; Cao, F.; Wang, K.; Lv, X.; Song, Q.; Zhang, C.; Zhao, S.; Lv, C. *Angew. Chem. Int. Ed.* **2021,** *60*, 1-6.

(5) (a) Hu, J.-X.; Xu, Y.; Meng, Y.-S.; Zhao, L.; Hayami, S.; Sato, O.; Liu, T. *Angew. Chem.* **2017,** *129*, 13232-13235; (b) Lama, P.; Hazra, A.; Barbour, L.J. *Chem. Commun.* **2019,** *55*, 12048-12051.

(6) (a) Mei, J.; Leung, N.L.C.; Kwok, R.T.K.; Lam, J.W.Y.; Tang, B.Z. *Chem. Rev.* **2015,** *115*, 11718-11940; (b) Huang, Y.; Xing, J.; Gong, Q.; Chen, L.-C.; Liu, G.; Yao, C.; Wang, Z.; Zhang, H.-L.; Chen, Z.; Zhang, Q. *Nat. Commun.* **2019,** *10*, 1-9.

(7) (a) Tan, Y.-Z.; Yang, B.; Parvez, K.; Narita, A.; Osella, S.; Beljonne, D.; Feng, X.; Müllen, K. *Nat. Commun.* **2013,** *4*, 1-7; (b) Hu, Y.; Xie, P.; De Corato, M.; Ruini, A.; Zhao, S.; Meggendorfer, F.; Straasø, L.A.; Rondin, L.; Simon, P.; Li, J.; Finley, J.J.; Hansen, M.R.; Lauret, J.-S.; Molinari, E.; Feng, X.; Barth, J.V.; Palma, C.-A.; Prezzi, D.; Müllen, K.; Narita, A. *J. Am. Chem. Soc.* **2018,** *140*, 7803-7809; (c) Zhu, Y.; Guo, X.; Li, Y.; Wang, J. *J. Am. Chem. Soc.* **2019,** *141*, 5511-5517.

(8) (a) Gingras, M. *Chem. Soc. Rev.* **2013,** *42*, 968-1006; (b) Gingras, M.; Félix, G.; Peresutti, R. *Chem. Soc. Rev.* **2013,** *42*, 1007-1050; (c) Gingras, M. *Chem. Soc. Rev.* **2013,** *42*, 1051-1095; (d) Shen, Y.; Chen, C.-F. *Chem. Rev.* **2012,** *112*, 1463-1535.

(9) Coe, B.J.; Rusanova, D.; Joshi, V.D.; Sánchez, S.; Vávra, J.; Khobragade, D.; Severa, L.s.; Císařová, I.; Šaman, D.; Pohl, R.; Clays, K.; Depotter, G.; Brunschwig, B.S.; Teplý, F. *J. Org. Chem.* **2016,** *81*, 1912-1920.

(10) (a) Yang, Y.; Da Costa, R.C.; Fuchter, M.J.; Campbell, A.J. *Nat. Photon.* **2013,** *7*, 634-638; (b) Rice, B.; LeBlanc, L.M.; Otero-de-la-Roza, A.; Fuchter, M.J.; Johnson, E.R.; Nelson, J.; Jelfs, K.E. *Nanoscale* **2018,** *10*, 1865-1876; (c) Ren, M.; Wang, J.; Xie, X.; Zhang, J.; Wang, P. *ACS Energy Lett.* **2019,** *4*, 2683-2688; (d) Xu, N.; Zheng, A.; Wei, Y.; Yuan, Y.; Zhang, J.; Lei, M.; Wang, P. *Chem. Sci.* **2020,** *11*, 3418-3426; (e) Storch, J.; Zadny, J.; Strasak, T.; Kubala, M.; Sykora, J.; Dusek, M.; Cirkva, V.; Matejka, P.; Krbal, M.; Vacek, J. *Chem.-Eur. J.* **2015,** *21*, 2343-2347; (f) Kim, C.; Marks, T.J.; Facchetti, A.; Schiavo, M.; Bossi, A.; Maiorana, S.; Licandro, E.; Todescato, F.; Toffanin, S.; Muccini, M. *Org. Electron.* **2009,** *10*, 1511-1520.

(11) (a) Huang, Q.; Jiang, L.; Liang, W.; Gui, J.; Xu, D.; Wu, W.; Nakai, Y.; Nishijima, M.; Fukuhara, G.; Mori, T.; Inoue, Y.; Yang, C. *J. Org. Chem.* **2016,** *81*, 3430-3434; (b) Tounsi, M.; Ben Braiek, M.; Baraket, A.; Lee, M.; Zine, N.; Zabala, M.; Bausells, J.; Aloui, F.; Ben Hassine, B.; Maaref, A.; Errachid, A. *Electroanal.* **2016,** *28*, 2892-2899.

(12) (a) Kelly, T.R.; De Silva, H.; Silva, R.A. *Nature* **1999,** *401*, 150-152; (b) Brandt, J.R.; Salerno, F.; Fuchter, M.J. *Nat. Rev. Chem.* **2017,** *1*, 0045; (c) Suda, M.; Thathong, Y.; Promarak, V.; Kojima, H.; Nakamura, M.; Shiraogawa, T.; Ehara, M.; Yamamoto, H.M. *Nat. Commun.* **2019,** *10*, 1-7.

(13) Laarhoven, W.H.; Prinsen, W.J.C., Carbohelicenes and heterohelicenes. In *Stereochemistry*, Springer1984; pp 63-130.

(14) (a) Sapir, M.; Donckt, E.V. *Chem. Phys. Lett.* **1975,** *36*, 108-110; (b) Otani, T.; Tsuyuki, A.; Iwachi, T.; Someya, S.; Tateno, K.; Kawai, H.; Saito, T.; Kanyiva, K.S.; Shibata, T. *Angew. Chem. Int. Ed.* **2017,** *56*, 3906-3910.

(15) (a) Dhbaibi, K.; Favereau, L.; Crassous, J. *Chem. Rev.* **2019,** *119*, 8846-8953; (b) Collins, S.K.; Vachon, M.P. *Org. Biomol. Chem.* **2006,** *4*, 2518-2524; (c) Schmidt, K.; Brovelli, S.; Coropceanu, V.; Beljonne, D.; Cornil, J.; Bazzini, C.; Caronna, T.; Tubino, R.; Meinardi, F.; Shuai, Z.; Brédas, J.-L. *J. Phys. Chem. A* **2007,** *111*, 10490-10499; (d) Yen-Pon, E.; Champagne, P.A.; Plougastel, L.; Gabillet, S.; Thuéry, P.; Johnson, M.; Muller, G.; Pieters, G.; Taran, F.; Houk, K.N.; Audisio, D. *J. Am. Chem. Soc.* **2019,** *141*, 1435-1440.

(16) (a) Sun, M.; Müllen, K.; Yin, M. *Chem. Soc. Rev.* **2016,** *45*, 1513-1528; (b) Chen, S.; Slattum, P.; Wang, C.; Zang, L. *Chem. Rev.* **2015,** *115*, 11967-11998; (c) Qin, Y.; Li, G.; Qi, T.; Huang, H. *Mater. Chem. Front.* **2020,** *4*, 1554-1568.

(17) (a) Gopikrishna, P.; Meher, N.; Iyer, P.K. *ACS Appl. Mater. Inter.* **2018,** *10*, 12081-12111; (b) Zhang, F.; Ma, Y.; Chi, Y.; Yu, H.; Li, Y.; Jiang, T.; Wei, X.; Shi, J. *Sci. Rep.* **2018,** *8*, 1-11; (c) Dayneko, S.; Cieplechowicz, E.; Bhojgude, S.; Van Humbeck, J.F.; Pahlevani, M.; Welch, G.C. *Mater. Adv.* **2021,** *2*, 933-936.

(18) Sakai, H.; Kubota, T.; Yuasa, J.; Araki, Y.; Sakanoue, T.; Takenobu, T.; Wada, T.; Kawai, T.; Hasobe, T. *J. Phys. Chem. C* **2016,** *120*, 7860-7869.

(19) Saal, F.; Zhang, F.; Holzapfel, M.; Stolte, M.; Michail, E.; Moos, M.; Schmiedel, A.; Krause, A.-M.; Lambert, C.; Wurthner, F.; Ravat, P. *J. Am. Chem. Soc.* **2020,** *142*, 21298-21303.

(20) (a) Yoon, S.-J.; Chung, J.W.; Gierschner, J.; Kim, K.S.; Choi, M.-G.; Kim, D.; Park, S.Y. *J. Am. Chem. Soc.* **2010,** *132*, 13675-13683; (b) Wang, C.; Li, Z. *Mater. Chem. Front.* **2017,** *1*, 2174-2194; (c) Gong, Y.-B.; Zhang, P.; Gu, Y.-r.; Wang, J.-Q.; Han, M.-M.; Chen, C.; Zhan, X.-J.; Xie, Z.-L.; Zou, B.; Peng, Q.; Chi, Z.-G.; Li, Z. *Adv. Opt. Mater.* **2018,** *6*, 1800198.

(21) (a) Berezhnaia, V.; Roy, M.; Vanthuyne, N.; Villa, M.; Naubron, J.-V.; Rodriguez, J.; Coquerel, Y.; Gingras, M. *J. Am. Chem. Soc.* **2017,** *139*, 18508-18511; (b) Zhao, L.; Kaiser, R.I.; Xu, B.; Ablikim, U.; Lu, W.; Ahmed, M.; Evseev, M.M.; Bashkirov, E.K.; Azyazov, V.N.; Zagidullin, M.V.; Morozov, A.N.; Howlader, A.H.; Wnuk, S.F.; Mebel, A.M.; Joshi, D.; Veber, G.; Fischer, F.R. *Nat. Commun.* **2019,** *10*.

(22) (a) Scholl, R.; Seer, C.; Weitzenböck, R. *Ber. Dtsch. Chem. Ges.* **1910,** *43*, 2202-2209; (b) Grzybowski, M.; Skonieczny, K.; Butenschön, H.; Gryko, D.T. *Angew. Chem. Int. Ed.* **2013,** *52*, 9900-9930.

(23) (a) Schuster, N.J.; Paley, D.W.; Jockusch, S.; Ng, F.; Steigerwald, M.L.; Nuckolls, C. *Angew. Chem. Int. Ed.* **2016,** *55*, 13519-13523; (b) Schuster, N.J.; Joyce, L.A.; Paley, D.W.; Ng, F.; Steigerwald, M.L.; Nuckolls, C. *J. Am. Chem. Soc.* **2020,** *142*, 7066-7074; (c) Weiss, C.; Sharapa, D.I.; Hirsch, A. *Chem.-Eur. J.* **2020,** *26*, 14100-14108.

(24) Navaza, J.; Tsoucaris, G.; Le Bas, G.; Navaza, A.; De Rango, C. *Bulletin des Sociétés Chimiques Belges* **1979,** *88*, 863-870.

(25) Isobe, H.; Matsuno, T.; Hitosugi, S.; Nakanishi, W. *Acta Crystallogr. E* **2012,** *68*, o1239-o1239.

(26) Bedard, A.-C.; Vlassova, A.; Hernandez-Perez, A.C.; Bessette, A.; Hanan, G.S.; Heuft, M.A.; Collins, S.K. *Chem.-Eur. J.* **2013,** *19*, 16295-16302.

(27) Dracinsky, M.; Storch, J.; Cirkva, V.; Cisarova, I.; Sykora, J. *Phys. Chem. Chem. Phys.* **2017,** *19*, 2900-2907.

(28) Fuchter, M.J.; Weimar, M.; Yang, X.; Judge, D.K.; White, A.J.P. *Tetrahydron Lett.* **2012,** *53*, 1108-1111.

(29) (a) Lavigueur, C.; Foster, E.J.; Williams, V.E. *J. Am. Chem. Soc.* **2008,** *130*, 11791-11800; (b) Nakanishi, W.; Matsuno, T.; Ichikawa, J.; Isobe, H. *Angew. Chem. Int. Ed.* **2011,** *50*, 6048-6051; (c) Matsuno, T.; Kogashi, K.; Sato, S.; Isobe, H. *Org. Lett.* **2017,** *19*, 6456-6459; (d) Psutka, K.M.; LeDrew, J.; Taing, H.; Eichhorn, S.H.; Maly, K.E. *J. Org. Chem.* **2019,** *84*, 10796-10804.

(30) (a) Reichardt, C. *Chem. Rev.* **1994,** *94*, 2319-2358; (b) Pavlovich, V.S. *ChemPhysChem* **2012,** *13*, 4081; (c) Li, M.; Yao, W.; Chen, J.-D.; Lu, H.-Y.; Zhao, Y.; Chen, C.-F. *J. Mater. Chem. C* **2014,** *2*, 8373-8380.

(31) Hu, J.-Y.; Paudel, A.; Seto, N.; Feng, X.; Era, M.; Matsumoto, T.; Tanaka, J.; Elsegood, M.R.; Redshaw, C.; Yamato, T. *Org. Biomol. Chem.* **2013,** *11*, 2186-2197.

(32) Nagura, K.; Saito, S.; Yusa, H.; Yamawaki, H.; Fujihisa, H.; Sato, H.; Shimoikeda, Y.; Yamaguchi, S. *J. Am. Chem. Soc.* **2013,** *135*, 10322-10325.

(33) (a) Chi, Z.; Zhang, X.; Xu, B.; Zhou, X.; Ma, C.; Zhang, Y.; Liu, S.; Xu, J. *Chem. Soc. Rev.* **2012,** *41*, 3878-3896; (b) Xu, J.; Chi, Z., *Mechanochromic Fluorescent Materials: Phenomena, Materials and Applications*. Royal Society of Chemistry **2014**.